Available online at www.sciencedirect.com

SciVerse ScienceDirect

journal homepage: www.elsevier.com/locate/watres

Graphical Abstract

Water Research 2013, ■, ■■■

Effect of polydispersity on natural organic matter transport

Q1 **Lindsay A. Seders Dietrich, Daniel P. McInnis, Diogo Bolster, Patricia A. Maurice***

Department of Civil and Environmental Engineering and Earth Sciences, University of Notre Dame, 156 Fitzpatrick Hall, Notre Dame, IN 46556, USA

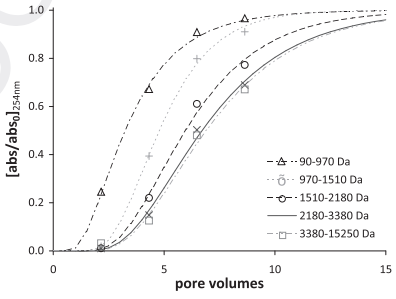

Highlights

► Preferential adsorption of NOM subcomponents caused tailing of breakthrough curves. ► Differences in retardation of NOM components were quantified for different MW ranges. ► Greater overall retardation of NOM was observed at low pH and high ionic strength. ► Adsorptive fractionation of NOM was slightly enhanced by Cd(II) in solution.

0043-1354/$ – see front matter © 2013 Published by Elsevier Ltd.
http://dx.doi.org/10.1016/j.watres.2013.01.053

WATER RESEARCH XXX (2013) 1–10

Available online at www.sciencedirect.com

SciVerse ScienceDirect

journal homepage: www.elsevier.com/locate/watres

Effect of polydispersity on natural organic matter transport

Lindsay A. Seders Dietrich [1], Daniel P. McInnis, Diogo Bolster, Patricia A. Maurice*

Department of Civil and Environmental Engineering and Earth Sciences, University of Notre Dame, 156 Fitzpatrick Hall, Notre Dame, IN 46556, USA

ARTICLE INFO

Article history:
Received 31 August 2012
Received in revised form
24 January 2013
Accepted 25 January 2013
Available online xxx

Keywords:
Column experiments
NOM
Molecular weight
Adsorption

ABSTRACT

The mobility of humic-substance dominated natural organic matter (NOM) concentrated from a freshwater wetland by reverse osmosis was examined in sand columns at pH 5–8, in 0.001 M and 0.01 M $NaClO_4$. Greater mobility was observed at higher pH and lower ionic strength, although breakthrough curves (BTCs) for bulk NOM exhibited extensive tailing under all conditions examined. Based on observations from previous batch experiments indicating preferential adsorption of intermediate to high molecular weight (MW) NOM, we postulate that 'adsorptive fractionation' of the NOM pool leads to the observed tailing behavior, and develop a novel approach to assess the effects of polydispersity on transport of NOM and associated contaminants. BTCs for different NOM fractions were constructed by separating column effluent MW distributions determined by high-pressure size exclusion chromatography into five discrete intervals or 'bins' and calculating the mass of NOM within each bin at four sampling times. Observed retardation factors (R_o), reflecting median arrival time relative to that of a nonreactive tracer, ranged from 1.4 to 7.9 for the various bins and generally increased with MW. NOM retarded transport of the contaminant metal Cd (2.5 ppm, in 0.01 M $NaClO_4$) slightly at pH 5 and more substantially at pH 8. Although Cd had little or no effect on bulk NOM transport, retention of the more aromatic, IMW-HMW NOM appeared to be slightly enhanced by Cd. Study results demonstrate that heterogeneity in retardation as a function of MW is likely a major factor contributing to bulk NOM BTC tailing and may have important implications for contaminant transport.

1. Introduction

Natural organic matter (NOM) is ubiquitous in aquatic and terrestrial environments and influences transport of heavy metals (Bryan et al., 2005), radionuclides (McCarthy et al., 1998), and hydrophobic organic contaminants (Johnson and Amy, 1995). A quantitative understanding of NOM transport is thus essential for assessing potential contaminant mobility. Yet because NOM is a polydisperse mixture of molecules with a wide range of molecular weights (MWs), chemical compositions, and functional group identities and distributions (Aiken et al., 1985; Cabaniss et al., 2000), modeling of NOM transport is challenging.

NOM subsurface transport is controlled at least in part by sorption to the porous medium, which is influenced by such factors as: (1) mineral surface properties, (2) flow rate, (3) solution conditions such as NOM concentration, pH, ionic strength (I), and concentrations of multi-valent cations, and (4) the physicochemical characteristics of the NOM itself (e.g., Tipping, 1981; Vermeer et al., 1998; Avena and Koopal, 1999;

* *Corresponding author*. Tel.: +1 574 631 3469; fax: +1 574 631 9236.
E-mail address: pmaurice@nd.edu (P.A. Maurice).
[1] Current address: Department of Civil and Environmental Engineering, Southern Methodist University, P.O. Box 750340, Dallas, TX 75275, USA.

0043-1354/$ – see front matter © 2013 Published by Elsevier Ltd.
http://dx.doi.org/10.1016/j.watres.2013.01.053

Namjesnik-Dejanovic et al., 2000; Zhou et al., 2001; Hur and Schlautman, 2003; Maurice et al., 2004; Weng et al., 2006; Maurice, 2009). The various components of NOM display a range of adsorption rates and affinities as determined largely by MW (e.g., Meier et al., 1999; Namjesnik-Dejanovic et al., 2000; Cabaniss et al., 2000; Zhou et al., 2001; Hur and Schlautman, 2003), although other factors (at least some of which often correlate with MW) including aromaticity, carboxyl group content, and amino acid residues can also be important (McKnight et al., 1992). Preferential adsorption of intermediate to high MW components can lead to different average properties of NOM in the dissolved versus adsorbed phases (e.g., Meier et al., 1999; Namjesnik-Dejanovic et al., 2000; Zhou et al., 2001; Hur and Schlautman, 2003; Pullin et al., 2004), a process often termed 'adsorptive fractionation' (McKnight et al., 1992). Adsorptive fractionation can involve both kinetic and thermodynamic (stability) effects; for example, Zhou et al. (2001) observed in batch studies of fulvic acid adsorption on goethite that lower MW (LMW) components adsorbed quickly but were gradually replaced by intermediate to higher MW (IMW-HMW) components. This has important implications for contaminant mobility because various NOM components differ in their abilities to bind and transport contaminants (Cabaniss et al., 2000).

In both column experiments and field studies, breakthrough curves (BTCs) for bulk NOM are characterized by an initial steep rise followed by extensive tailing, suggesting rapid breakthrough of certain NOM components followed by slow breakthrough of others (e.g., Dunnivant et al., 1992; McCarthy et al., 1996). BTCs with such extensive tailing cannot be fit by the classical advection dispersion equation (ADE) – the 'textbook' standard for solute transport in saturated porous media – which assumes linear, equilibrium adsorption of a single solute. A variety of modifications can be made to the ADE to model NOM BTC tailing; to date, most efforts have focused on the effects of heterogenous adsorption kinetics using parameters determined from batch experiments. One approach treats NOM as an essentially homogenous solute and accounts for adsorption heterogeneity by postulating two different types of adsorption sites with fast versus slow kinetics (Jardine et al., 1992; Dunnivant et al., 1992; McCarthy et al., 1993, 1996). In another approach (e.g., van de Weerd et al., 1999, 2002), the porous medium is modeled with a single type of adsorption site, and competitive adsorption parameters calculated for several NOM fractions are incorporated into a transport code.

Here, we demonstrate an alternative approach to assess whether BTC tailing may arise from heterogeneity in the adsorption affinities of different NOM MW intervals. Column experiments were conducted using a naturally Fe- and Al-oxide coated quartz sand and an NOM sample previously shown to undergo adsorptive fractionation to goethite (*á*-FeOOH) in batch experiments (Pullin et al., 2004). Transport was investigated at pH 5–8 in 0.001 M and 0.01 M $NaClO_4$. NOM MW distributions of column influent and of effluent at various times were measured and the transport rates of each MW interval calculated directly from resulting data. The primary objective of this study was to quantify the mobilities of different NOM fractions over a range of experimental conditions and thus determine whether BTC tailing might result, at least in part, from NOM polydispersity. A secondary objective was to determine the effects of NOM and of the contaminant metal Cd(II) on one another's mobility.

2. Materials & methods

2.1. Natural organic matter

NOM was concentrated on-site from surface water at Nelson's Creek, a first-order stream in the Ottawa National Forest (MI, USA), using a portable RealSoft PROS/1S reverse osmosis (RO) system (Sun et al., 1995). The physicochemical properties of the RO concentrate and of raw filtered water collected simultaneously were compared by Pullin et al. (2004) and are summarized in Table S1 in the supplementary data (SD). The weight and number average molecular weights (M_w and M_n, respectively) are higher for the RO concentrate than for the bulk water, likely reflecting removal of low molecular weight components and/or potential condensation or coagulation on the RO membranes as suggested by Maurice et al. (2002). Although the values of M_w, M_n, and the polydispersity ($\tilde{n}$) are consistent with those of aquatic fulvic acids (e.g., Chin et al., 1994), we use the more general term NOM because the humic fractions are strictly (operationally) defined by XAD resin isolation (Aiken et al., 1985).

2.2. Geosorbent

Columns were packed with naturally Fe/Al-oxide coated quartz sand from the U.S. Department of Energy research site in Oyster, Virginia (hereafter referred to as the Oyster sand). Characteristics of this sand are described by Dong et al. (2002) and in the SD. This geosorbent was chosen because many quartz sands contain coatings that enhance NOM adsorption relative to that of 'pure' quartz surfaces (e.g., Chi and Amy, 2004; Wei et al., 2010). The sand was dry sieved with a 20–40 mesh sieve (0.842–0.420 mm), rinsed repeatedly with distilled, deionized water (DDI), and dried overnight at 55 °C. Because the sand did not contain internal porosity, we shall refer to NOM sorption as 'adsorption' and assume no 'absorption.'

2.3. Column experiments

The limited supply of NOM constrained the column size, number and breadth of experiments, and number of replicate experiments. Columns consisted of a borosilicate glass barrel 10 cm long with 1.0 cm inner diameter (Kimble–Kontes; Vineland, NJ) and were rinsed repeatedly with DDI water, then acetone, and dried at 60 °C prior to each use. Columns were wet packed by filling with background electrolyte and slowly adding sand grains while tapping gently to remove air bubbles. Porosity was calculated from column weight under dry versus saturated conditions. A gravity-feed system passed solutions through the stationary sand grains at a constant flow rate of ~2 mL/min 20–25 mL (~6–7 pore volumes) of background electrolyte was passed through the column prior to introducing the experimental solution. All column experiments were repeated in duplicate.

Please cite this article in press as: Seders Dietrich, L.A., et al., Effect of polydispersity on natural organic matter transport, Water Research (2013), http://dx.doi.org/10.1016/j.watres.2013.01.053

Freeze-dried Nelson's Creek RO concentrate was combined with deionized (MilliQ) water and vacuum filtered through a 0.45 μm polycarbonate membrane filter to make an NOM stock solution. NOM sample solutions (5 ppm C; pH 5, 6, 7, 8) were then prepared by mixing $NaClO_4$ (0.001 M or 0.01 M) background solutions with the NOM stock. Solution pH was adjusted with HCl and/or NaOH. The non-adsorbing conservative tracer sulforhodamine B (Sigma–Aldrich; St. Louis, MO) was used at both ionic strengths and pH 5 and 8. Similar experiments were run to determine the effects of NOM (0, 5, and 20 ppm C) on Cd transport at pH 5 and 8, in 0.01 M $HClO_4$. Cd solutions (2.5 ppm) were prepared from 1000 ppm Cd ICP stock in 2% HCl (Fisher Scientific; Pittsburgh, PA).

2.4. Solution analysis

For initial/influent and final effluent solutions, UV/visible absorbance (λ = 200–600 nm) was measured using a Varian Cary 3 spectrophotometer with 1.0 cm quartz cells; dissolved organic carbon concentration ([DOC]) of a subset of samples was measured using a Shimadzu TOC5000. In-line measurements of [DOC] were not conducted, because the analyzer in our lab tends to require relatively large samples at low [DOC] (as described in Kreller et al., 2005), making continuous measurements impossible for small columns. Effluent NOM was monitored continuously using an in-line (Hewlett Packard 8453) UV/Vis spectrophotometer at λ = 254 nm, a wavelength that has been broadly used as a surrogate for [DOC] in humic-rich waters (such as studied here; Dobbs et al., 1972), and that tends to be highly sensitive and reproducible for small samples at low [DOC], as occur at the earliest times of BTCs. Absorbance at 565 nm was used to monitor the non-reactive tracer sulforhodamine B. Effluent absorbance values were normalized to the absorbance of the influent solution, and BTCs for NOM and tracer solutions were constructed by plotting the normalized absorbance (abs/abs_0) versus the number of pore volumes (dimensionless) eluted from the column.

Retention of NOM in the columns is discussed in terms of the observed retardation factor (R_o), equal to the number of pore volumes at which $[abs/abs_0]_{254nm}$ = 0.5 (50% retention; e.g., Liu and Amy, 1993). Precise estimates of R_o were obtained by linear interpolation between the nearest data points above and below the 50% retention mark. Values of R_o averaged across repeat experiments are denoted by $\overline{R}_o$.

Subsamples (5 mL and 1.5 mL) of column influent and effluent (after passing through the in-line spectrophotometer) were collected for further analysis. Inductively coupled plasma-optical emission spectrometry (ICP-OES; Perkin Elmer Optima 2000 DV) was used to determine [Cd]. NOM MW distributions were determined by high-pressure size exclusion chromatography (HPSEC; Waters 2695 HPLC system, Waters Protein Pak 125 modified silica column, 0.1 M NaCl mobile phase; detection at 254 nm by Waters 2996 photodiode array) following Chin et al. (1994) and Zhou et al. (2000). Although several studies have suggested that in-line [DOC] detection on HPSEC can be important for some NOM samples (e.g., Huber and Frimmel, 1992; Frimmel and Huber, 1996; Huber et al., 2011; Kawasaki et al., 2011), previous research by our group suggested that UV/vis detection (λ = 254 nm) was appropriate for the RO concentrate used here (Kreller et al., 2005). For our HPSEC system, in-line detection by UV/vis requires smaller samples and provides greater reproducibility and sensitivity than [DOC] detection.

MW distributions of column influent and effluent were determined from HPSEC retention time using acetone (Aldrich, 58 Da), salicylate (Aldrich, 138 Da), and polystyrene sulfonate (PSS) polymers from Polysciences, Inc. (1430 Da; 4950 Da; 6530 Da; 15,200 Da) as calibration standards (Zhou et al., 2000). The MW distribution (mass vs. $\log_{10}$ MW) of NOM retained in the columns at each time period was then calculated as:

$$m\left[\log_{10}(\mathrm{MW}), t_i\right]_{\mathrm{retained}} = m\left[\log_{10}(\mathrm{MW})\right]_{\mathrm{influent}} - m\left[\log_{10}(\mathrm{MW}), t_i\right]_{\mathrm{effluent}} \quad (1)$$

where m is mass of NOM in solution (measured as absorbance), MW is molecular weight, and t_i denotes one of the four sampling intervals. The distributions of NOM retained in the column at each sampling period were compared to the MW distribution of the influent solution. The weight average MW (M_w; calculated as by Cabaniss et al. (2000), Zhou et al. (2000) of influent and effluent solutions were also compared.

2.5. Determination of MW bins

To calculate the differences in transport rates between NOM MW fractions, the area under the HPSEC curve for the influent NOM solution was divided into five intervals of equal mass. The chromatogram was first truncated using a LMW cutoff of 50 Da or 2% of the maximum absorbance (whichever is higher), and a HMW cutoff of 1% of the maximum absorbance, as recommended by Zhou et al. (2000). Assuming a log-normal distribution model, as proposed by Cabaniss et al. (2000) (and demonstrated by our data – see Section 3.4), the mean (μ_m) and standard deviation (σ) of the NOM mass distribution were determined by fitting the HPSEC chromatogram (abs_{254nm} vs. $\log_{10}$(MW)) using a Gaussian peak shape. The mass $m_{(a,\ b)}$ within MW range (M_a, M_b) was then calculated from the log-normal cumulative distribution function (CDF):

$$m_{(a,b)} = \frac{1}{\sigma\sqrt{2\pi}} \int_{M_a}^{M_b} \frac{1}{\mathrm{MW}} \exp\left(\frac{-\left(\log_{10}(\mathrm{MW}) - \mu_m\right)^2}{2\sigma^2}\right) d(\mathrm{MW}) = \frac{1}{2}\left[erf\left(\frac{\log_{10(M_a)} - \mu_m}{\sigma\sqrt{2\pi}}\right) - erf\left(\frac{\log_{10(M_b)} - \mu_m}{\sigma\sqrt{2\pi}}\right)\right] \quad (2)$$

where $erf(x)$ denotes the error function. Normalized BTCs for each MW interval were constructed by normalizing the effluent chromatogram to the CDF of the influent solution at each of four sampling times and used to determine R_o for each MW interval.

3. Results and discussion

3.1. Tracer and bulk NOM BTCs

Conservative tracer and NOM BTCs (abs/abs_0 vs. pore volumes eluted) are presented in Figs. 1 and 2, and values of R_o for duplicate experiments ('a' and 'b') are given in Table 1. The average $\overline{R}_o$ = 1.0 for the conservative tracer, which is expected

Please cite this article in press as: Seders Dietrich, L.A., et al., Effect of polydispersity on natural organic matter transport, Water Research (2013), http://dx.doi.org/10.1016/j.watres.2013.01.053

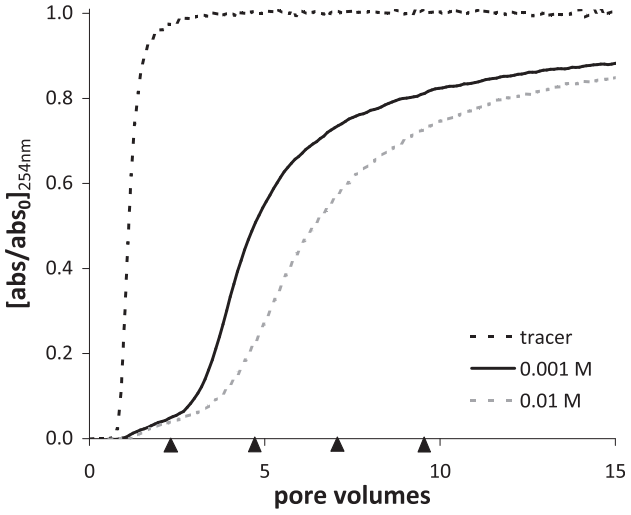

Fig. 1 – NOM retention on Oyster sand increased as a function of background electrolyte ($NaClO_4$) concentration at pH 5. Black dashed line: conservative tracer (0.01 M, pH 5a); black solid line: 0.001 M, pH 5a; gray dashed line: 0.01 M, pH 5b. Arrows along the horizontal axis represent effluent sampling times for HPSEC analysis.

for a non-reactive solute. NOM solutions all showed greater retention than the tracer ($R_o \geq 1.5$). NOM retention increased with increasing I; for the data at pH 5 (Fig. 1), $\overline{R}_o = 4.7$ for 0.001 M and 5.9 for 0.01 M $NaClO_4$, respectively. Retention also decreased with increasing pH (Fig. 2): in 0.001 M $NaClO_4$, $\overline{R}_o = 4.7$, 2.7, 2.0, and 1.5 pore volumes for pH 5, 6, 7 and 8, respectively.

The classical ADE model provides an excellent fit to the experimental BTCs for the sulforhodamine B tracer (average $r^2 = 0.9986$; Fig. 3a). However, BTCs for bulk NOM displayed significant retardation and tailing at late times that could not be captured by this model (Fig. 3b). For this reason, ADE model parameters are not presented here. The failure of the ADE model to capture BTC tailing is attributed to NOM polydispersity, as discussed in Section 3.5.

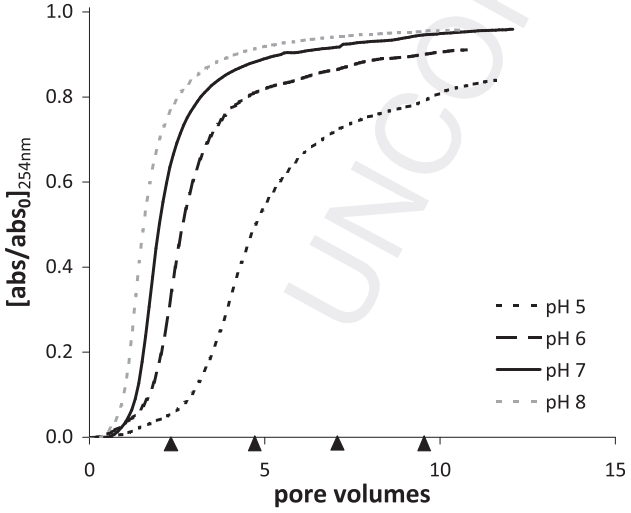

Fig. 2 – NOM retention at 0.001 M as a function of pH (data plotted are pH 5a, 6b, 7b, and 8b). Overall retention decreases with increasing pH. Arrows along the horizontal axis represent effluent sampling times for HPSEC analysis.

Table 1 – Summary of BTCs for bulk NOM and sulforhodamine B tracer under various solution conditions in experiments with and without Cd.

	I [M $NaClO_4$]	pH	Flow rate [mL/min]	Pore volume [cm^3]	R_o
NOM only	0.001	5a	2.0	3.4	4.9
		5b	2.0	3.3	4.7
	0.001	6a	2.0	3.3	2.7
		6b	2.0	3.2	2.7
	0.001	7a	2.0	3.4	2.0
		7b	2.0	3.3	2.0
	0.001	8a	2.0	3.3	1.5
		8b	2.0	3.2	1.5
	0.01	5a	2.0	3.5	5.9
		5b	2.0	3.5	5.9
	0.01	6a	2.0	3.5	5.1
		6b	2.0	3.5	5.1
	0.01	7a	2.0	3.4	4.4
		7b	2.0	3.1	4.4
	0.01	8a	2.0	3.3	4.0
		8b	2.0	3.4	4.0
NOM + Cd	0.01	5a	1.9	3.4	5.7
		5b	1.8	3.6	5.2
	0.01	6a	1.7	3.6	4.9
		6b	2.0	3.5	4.8
	0.01	7a	2.0	3.6	3.8
		7b	1.8	3.5	4.1
	0.01	8a	2.1	3.4	3.8
		8b	2.0	3.3	3.1
Tracer	0.01	5a	2.0	3.4	1.1
		5b	2.1	3.3	1.0
	0.01	8a	1.8	3.4	1.0
		8b	2.0	3.4	0.8

3.2. *Bulk NOM retention*

Observed retardation factors for bulk NOM transport under the range of experimental conditions examined are summarized in Table 1. Under all conditions examined, R_o values are consistently much greater for NOM than for the tracer, indicating that adsorption (and/or desorption) reactions strongly affect NOM mobility ($R_o = 1.5–5.9$). NOM retention is attributed to adsorption onto the column sands rather than to degradation and/or straining because: 1) experiments were short in duration, limiting potential for microbial activity which could lead to NOM degradation; 2) previous batch and column experiments have demonstrated adsorption of NOM onto mineral surfaces (e.g., Tipping, 1981; Dunnivant et al., 1992; Gu et al., 1996; Meier et al., 1999; Namjesnik-Dejanovic et al., 2000; Zhou et al., 2001; Guo and Chorover, 2003; Chi and Amy, 2004); and 3) experiments performed in flow-through columns using an uncoated quartz sand and various NOM samples resulted in little retention of NOM (Weigand and Totsche, 1998; Wei et al., 2010).

Observations of decreased retention (hence lower R_o; Table 1, Fig. 2) with increasing pH agree with results of

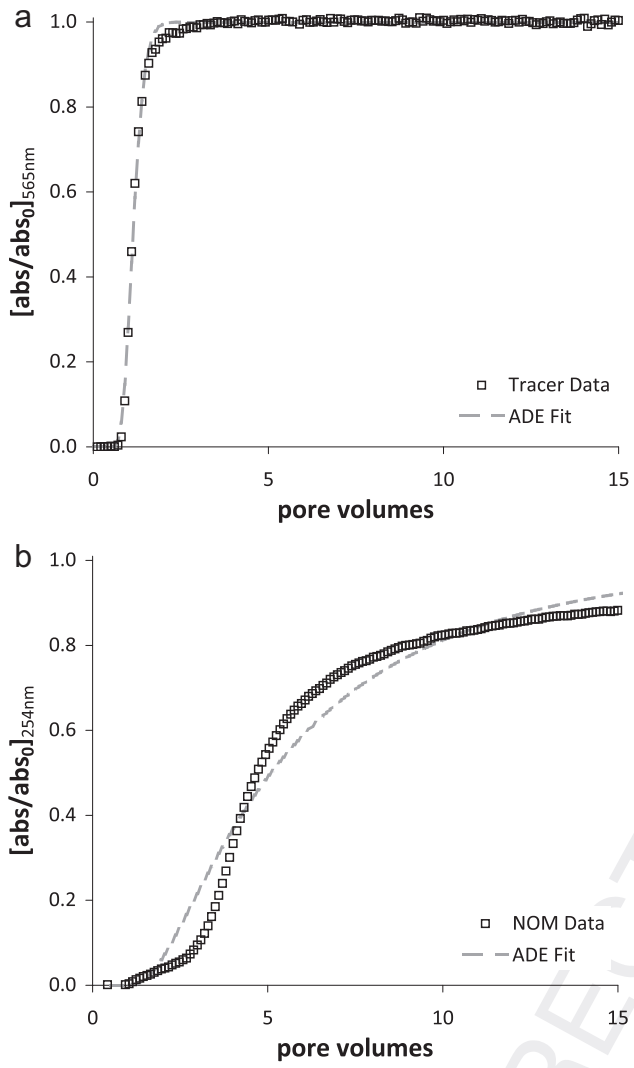

Fig. 3 – Advection–dispersion equation (ADE) fit to experimental breakthrough curves (BTCs) for the non-reactive tracer sulforhodamine B (0.01 M, pH 5a; a) and for NOM (0.001 M, pH 5a; b). While the best-fit ADE model provides a near-perfect match to the tracer data, the NOM data show strong tailing at late times that is not captured well by the ADE model.

previous batch studies showing that NOM adsorption affinity tends to decrease with increasing pH (e.g., Tipping, 1981; Vermeer et al., 1998; Zhou et al., 2001). Retention was also enhanced at higher *I* (Table 1, Fig. 1). In batch experiments, humic acid adsorption to Fe/Al-oxides has been shown to increase with increasing *I* (Schlautman and Morgan, 1994; Vermeer et al., 1998; Filius et al., 2000; Münch et al., 2002; Saito et al., 2004; Weng et al., 2006), whereas studies of *I* effects on fulvic acid adsorption have produced mixed results (Schlautman and Morgan, 1994; Filius et al., 2000; Weng et al., 2006). It is likely that a combination of the effects of surface charge, charge screening, NOM hydrophobicity, and/or conformational changes governs NOM adsorption under different *I* conditions (e.g., Vermeer et al., 1998; Münch et al., 2002; Au et al., 1999; Pullin et al., 2004).

3.3. *Preferential retention of NOM components*

UV absorbance ratios and the MW distribution of NOM in the column effluent indicated preferential retention (due to preferential adsorption) of HMW, more aromatic NOM components. The initial 280 nm/254 nm ratio in the column effluent was less than that of the influent (~0.7 and 0.8, respectively; Fig. S1), indicating preferential retention of more aromatic components (Traina et al., 1990) and greater mobility of slightly less aromatic components. Other investigators have observed a decrease in the aromaticity or molar absorptivity at 280 nm of NOM remaining in solution in batch adsorption experiments (e.g., Dunnivant et al., 1992; McKnight et al., 1992; Zhou et al., 2001; Guo and Chorover, 2003; Pullin et al., 2004). Similarly, the M_w of NOM in the column effluent (Table 2) remained lower than that of the influent, indicating preferential retention of IMW-HMW components within the column. Decrease in NOM M_w upon adsorption has been observed in both batch and column experiments (e.g., Meier et al., 1999; Namjesnik-Dejanovic et al., 2000; Guo and Chorover, 2003; Pullin et al., 2004).

As the experiments progressed, overall NOM retention decreased, but preferential adsorption persisted. The peak of the MW distribution for NOM retained in the column (calculated from HPSEC data as the difference between influent and effluent chromatograms at each of four sampling times t_{1-4}) shifted toward lower maximum absorbance, but higher $\log_{10}$ MW (from 3.2 to 3.3 or 3.4 for the 0.001 M or 0.01 M experiments, respectively) over time. The 'retained' NOM MW distributions only reveal what is retained in the column at a particular point in time, thus may be masking transient effects of NOM adsorption exchange at the mineral surface

Table 2 – Weight average molecular weight, M_w (in Daltons), of influent and effluent NOM at t_{1-4} from column experiments with 5 ppm C in 0.001 M $NaClO_4$ and 0.01 M $NaClO_4$ with or without Cd.

pH 6		pH 8	
Sample	M_w	Sample	M_w
0.001 M–5 ppm C			
Influent	2030	Influent	1970
t_1	572	t_1	2090
t_2	2110	t_2	2040
t_3	2010	t_3	2030
t_4	2010	t_4	2050
0.01 M–5 ppm C			
Influent	2170	Influent	2280
t_1	411	t_1	699
t_2	1240	t_2	1900
t_3	1920	t_3	2120
t_4	2050	t_4	2200
0.01 M–5 ppm C + Cd			
Influent	2250	Influent	2290
T_1	509	t_1	522
T_2	1020	t_2	1640
T_3	1610	t_3	1980
T_4	1880	t_4	2070

Please cite this article in press as: Seders Dietrich, L.A., et al., Effect of polydispersity on natural organic matter transport, Water Research (2013), http://dx.doi.org/10.1016/j.watres.2013.01.053

that occur between sample points and cannot be inferred directly from these macroscopic measurements. Nevertheless, they provide a measure of the fraction of influent NOM retained (adsorbed) within the column and indicate how this distribution evolves over time.

At t_1, essentially all NOM components were retained, with only a small proportion of LMW material passing through the column, hence low effluent M_w (Fig. 4, Fig. S2). The 280 nm/254 nm absorbance ratio and M_w of the effluent gradually increased with time, approaching the influent absorbance ratio and M_w by t_4. These changes occurred more quickly at lower *I* and higher pH, suggesting that preferential adsorption of IMW-HMW components was more persistent under conditions at which more overall NOM adsorption occurred (Table 2).

These results are consistent with results of batch adsorption experiments on NOM adsorption to goethite (Zhou et al., 2001; Pullin et al., 2004) which showed that (1) a portion of LMW components did not adsorb under any conditions, and (2) 'adsorptive fractionation' increased as a function of surface coverage due to increased competition for surface sites. At high coverage, when sorbent molecules greatly exceeded available sorbent surface sites, greater competition favored adsorption of larger molecules. However, the very highest MW material did not adsorb preferentially at high surface coverages, perhaps due to increased electrostatic repulsion between these highly charged molecules and nearby adsorbed molecules, particularly at high solution pH. Conversely, at low pH, protonation promoted adsorption of HMW components by leading to less negatively charged molecules and likely stabilization via hydrophobic interactions.

Kinetic limitations might explain, at least in part, the lower adsorption affinity of the highest MW fraction in the column experiments. Competitive displacement during adsorption of polymers of different sizes has been well documented; similarly, fast-adsorbing LMW fractions of NOM may be successively replaced by slow-adsorbing HMW fractions (e.g., Gu et al., 1996). If this displacement does not achieve steady state, then adsorption of HMW fractions may be underestimated. Zhou et al. (2001) reported that fast-adsorbing LMW components of fulvic acid were replaced on goethite within a few minutes by larger components, which formed more stable adsorption complexes. At high surface coverages, even after attainment of apparent steady state (in terms of both total adsorbed DOC and MW distributions), lack of adsorption of the highest MW components persisted. Adsorption of HMW components may be inhibited by an interfacial electrostatic barrier that increases with molecular size, hence increased total molecular charge, as observed by de Laat and van den Heuvel (1995) for polyacrylic acid (PAA) at low salt concentrations.

3.4. NOM retardation as a function of MW

To quantify the different transport behaviors of the various NOM components (by MW), the MW distribution was divided into bins (Fig. 5). HPSEC chromatograms for all influent solutions exhibited a unimodal Gaussian peak [$\log_{10}(MW) \sim N(3.2, 0.3)$], although with some tailing on the LMW side of the peak. Cabaniss et al. (2000) observed similar tailing in experimentally determined MW distributions for aquatic fulvic acids and attributed the asymmetry to sorption interactions within the stationary phase of the HPSEC column. Despite the slight asymmetry, the chromatogram is well described as a log-normal MW distribution. Minor variability among the MW distributions of influent NOM solutions used in the experiments led to slight differences in the MW bins that divide the chromatogram into equal segments; average MW cutoffs are reported in Table 3.

Average R_o values for each of the MW bins are listed in Table 3. Although there are only four data points per bin (due to sampling constraints), trends in NOM component mobility similar to those observed for bulk NOM are clearly observed in the HPSEC data. Differences in $\overline{R}_o$ were observed across MW

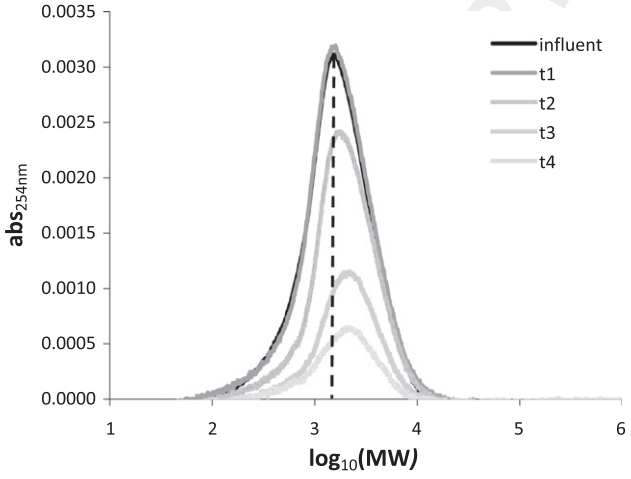

Fig. 4 – Molecular weight (MW) distributions of NOM retained in the column (calculated as the difference between column influent and effluent at a particular time *t*) for each of four sampling periods compared to the influent MW distribution from experiments conducted with 5 ppm C in 0.01 M $NaClO_4$, pH 6b. Dashed vertical line represents the MW peak of the influent solution.

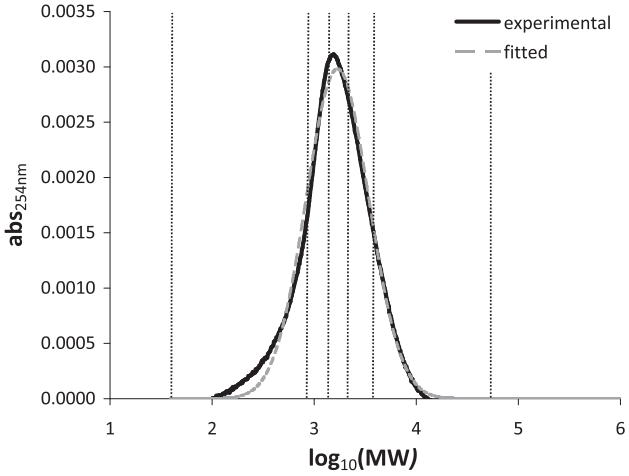

Fig. 5 – NOM MW distribution determined by HPSEC ('experimental'), and approximated by a log-normal model ('fitted'). Vertical lines separate the log-normal distribution into MW intervals of equal mass.

Please cite this article in press as: Seders Dietrich, L.A., et al., Effect of polydispersity on natural organic matter transport, Water Research (2013), http://dx.doi.org/10.1016/j.watres.2013.01.053

Table 3 – Average R_o for individual NOM MW fractions under various solution conditions. Average MW cutoffs between each of the five intervals are reported in Daltons (Da).

I[M $NaClO_4$]	pH	$\overline{R}_o$				
		MW1 [60–930 Da]	MW2 [930–1460 Da]	MW3 [1460–2130 Da]	MW4 [2130–3330 Da]	MW5[a] [>3330 Da]
0.001	5	3.4	4.6	5.5	5.8	5.0
	6	3.2	3.7	3.9	3.9	3.6
	7	1.4	1.8	2.2	2.0	1.6
	8	1.5	1.7	2.0	1.9	1.6
0.01	5	4.1	5.7	6.8	7.9	7.7
	6	3.5	5.0	5.9	6.6	6.8
	7	2.6	3.6	4.1	4.6	4.7
	8	2.8	3.6	4.1	4.6	4.8

a HMW cutoff = 1% of chromatogram peak height; values (not shown) vary due to tailing of HPSEC data.

intervals for a given set of experimental conditions. A one-way analysis of variance (ANOVA) revealed significant differences in retardation amongst the five MW bins (F_{crit} (4, 5) = 5.19, $p = 0.05$; see the SD for details). $\overline{R}_o$ was greatest for IMW-HMW fractions, consistent with previous observations of NOM adsorptive fractionation in batch experiments (Zhou et al., 2001; Hur and Schlautman, 2003; Pullin et al., 2004). Fig. 6 shows BTCs for all five MW bins at 0.01 M and pH 6. Similar patterns were observed for the other experiments (data not shown). As with the bulk NOM transport data, $\overline{R}_o$ for individual MW bins tended to decrease with increasing pH and to increase with increasing I. For example, $\overline{R}_o$ of MW2 decreased from 4.6 to 3.7, 1.8, and 1.7 at pH 5, 6, 7, and 8, respectively in 0.001 M $NaClO_4$ and from 5.7 to 5.0, 3.6, and 3.6 at the same pH values in 0.01 M $NaClO_4$.

3.5. *Effects of NOM polydispersity on BTC tailing*

Tailing of the bulk NOM BTCs cannot be attributed to variations in flow velocity within the porous medium, because tailing is not observed in the tracer BTCs (Fig. 3). Drawing on research in contaminant hydrology, which has shown that a broad range of retardation factors distributed randomly throughout a system can lead to BTC tailing (Dentz and Castro, 2009; Dentz and Bolster, 2010), and based on the observation of differences in retardation for different MW bins (Table 3), we attribute the bulk NOM BTC tailing to NOM geochemical heterogeneity. Although the cited studies focused on spatially variable retardation resulting from heterogeneity of the porous medium, the equivalence between spatial and ensemble averages (known as the 'ergodic' hypothesis; Dagan, 1990) implies that the same principle could be used to describe transport of an ensemble of NOM components each displaying a unique retardation factor.

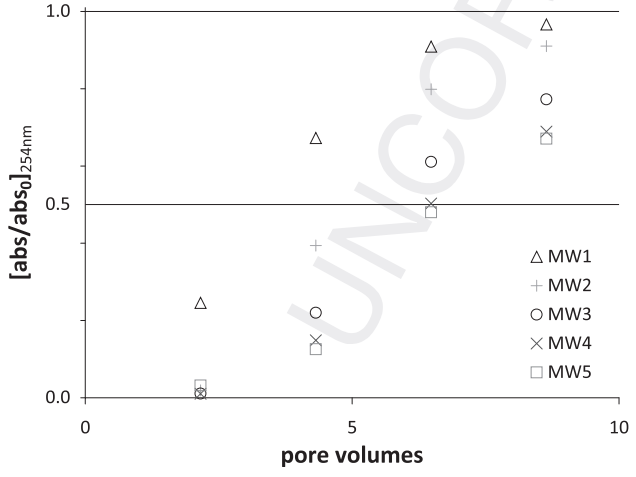

Fig. 6 – BTCs for NOM fractions of differing MW for experiments conducted at 0.01 M, pH 6b. Marker symbols indicate the proportion of the influent mass (measured as absorbance at 254 nm) within a particular MW range detected in the sand column effluent, as determined from HPSEC data at four sampling times.

3.6. *Effects of NOM on Cd and of Cd on NOM retention*

In the absence of organic ligands, Cd(II) adsorption to oxides and clays tends to follow an adsorption edge; i.e., adsorption increases with increasing pH (e.g., Johnson, 1990; Angove et al., 1997). In contrast, NOM adsorption to minerals tends to decrease with increasing pH (Tipping, 1981). Cd adsorption in ternary systems (metal-ligand-mineral surface) is difficult to predict, as the overall effect of NOM on Cd adsorption depends on numerous competing interactions (Davis and Bhatnagar, 1995). Cd adsorption can be decreased if NOM bound to mineral surfaces blocks adsorption sites and/or if formation of dissolved Cd-NOM complexes prevents a fraction of the metal from adsorbing. Alternatively, cationic Cd adsorption could be enhanced by formation of ternary surface complexes and/or by surface charge effects when negatively-charged NOM adsorbs to positively-charged oxide or clay surfaces (Vermeer et al., 1999). Previous studies have shown that organic ligands can enhance, inhibit, or have no effects on Cd adsorption to oxides and clays depending upon the nature of the ligand and the mineral surface, along with pH and Cd concentration (Floroiu et al., 2001; Bäckström et al., 2003; Hepinstall et al., 2005; Alessi and Fein, 2010).

In the present study, a general increase in Cd retardation (hence Cd adsorption) was observed with increasing NOM concentration (0, 5, and 20 ppm C) at pH 5 and 8 (Table 4, Fig. S3). Because [Cd] was measured in discrete effluent samples rather than continuously, not enough data points are available to assess potential effects of NOM on Cd BTC tailing. This topic warrants further investigation.

Please cite this article in press as: Seders Dietrich, L.A., et al., Effect of polydispersity on natural organic matter transport, Water Research (2013), http://dx.doi.org/10.1016/j.watres.2013.01.053

Table 4 – Summary of BTCs for Cd in experiments with various concentrations of NOM.

NOM [ppm C]	pH	Flow rate [mL/min]	Pore volume [cm^3]	R_o
0	5a	2.0	3.3	1.6
	5b	2.1	3.3	2.5
0	8a	2.1	3.3	4.2
	8b	2.0	3.3	4.4
5	5a	2.1	3.3	1.5
	5b	1.9	3.3	1.8
5	8a	2.0	3.3	6.2
	8b	1.9	3.2	6.7
20	5a	1.9	3.6	2.4
	5b	1.9	3.7	2.6
20	8a	2.1	3.6	4.4
	8b	2.0	3.6	4.5

Cd had little effect on bulk NOM retention. While R_o decreased slightly in the presence of Cd at pH 5 ($\overline{R}_o$ = 5.5, 5.9 with and without Cd, respectively) and at pH 8 ($\overline{R}_o$ = 3.4, 4.0), BTCs for each pair of experiments were nearly indistinguishable (Fig. 7). These results agree with the observations of Floroiu et al. (2001), who found that Cd did not affect PAA adsorption to aluminum oxide (α-Al_2O_3), and Vermeer at al. (1998, 1999), who observed that Cd (10^{-4} M) slightly enhanced the adsorption of purified Aldrich humic acid to hematite in batch experiments at pH 9, but had no significant effect at lower pH.

Although Cd only slightly affected bulk NOM retention, preferential adsorption of the more aromatic, IMW-HMW components was enhanced (Figs. S4, S5). MW distributions of adsorbed NOM compiled for the four sampling intervals displayed a more pronounced shift toward IMW-HMW components in the presence of Cd (Fig. 8) and the increase in effluent M_w occurred more slowly in 5 ppm C experiments with Cd than without Cd (Table 2). This was not an effect of increased overall NOM adsorption, hence increased competition, because NOM R_o values decreased slightly in the presence of Cd (Table 1). It may indicate that Cd binding to NOM is MW specific, as observed for many metals (Cabaniss et al., 2000).

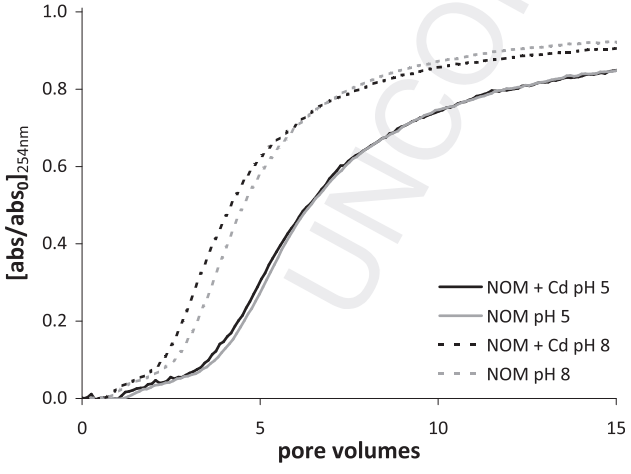

Fig. 7 – Effects of Cd (2.5 ppm) on NOM (5 ppm C) retention in Oyster sand. Cd slightly decreased NOM retention (presumably through effects on adsorption) onto Oyster sand in 0.01 M $NaClO_4$, pH 5a (solid lines) and pH 8a (dashed lines).

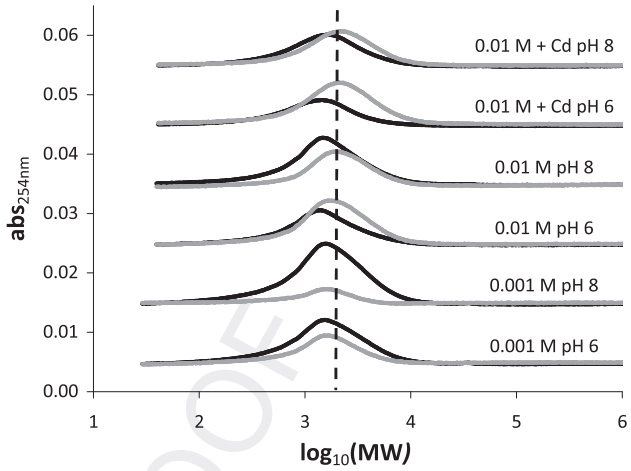

Fig. 8 – MW distributions of the 'total' effluent NOM (black lines) and 'total' adsorbed NOM (gray lines) compiled over the four HPSEC samples for each of the 5 ppm C experiments at pH 6 or 8 in 0.001 M $NaClO_4$ and 0.01 M $NaClO_4$ with or without Cd. The black vertical line represents the peak log MW of the influent solution.

4. Conclusions and implications

NOM consists of a mixture of organic molecules whose chemical behavior (e.g., hydrophobicity, affinity for metals and other contaminants, and adsorption affinity) strongly correlates with MW. Heterogeneity in NOM adsorption to porous media leads to strong BTC tailing that cannot be described by the classical ADE. Previous studies have relied on batch experiments to determine kinetic parameters to capture tailing in transport models. Here, we apply an alternative approach that uses analysis of column influent and effluent MW distributions to calculate observed retardation R_o for different MW intervals. Results demonstrate differences in the transport rates for NOM subcomponents, thus suggesting that NOM heterogeneity plays a clear role in tailing.

This research provides a new multi-component approach to conceptualizing NOM transport, which is needed to describe the complex behavior of such a heterogenous mixture. By determining transport rates not just for the bulk NOM sample, but for its individual components, we should ultimately be able to understand and model transport of contaminants and/or nutrients preferentially associated with different NOM fractions. The newly quantified retardation factors for different NOM components also set the stage for our group's ongoing research applying a new generation of anomalous transport models designed to address heterogeneity, such as continuous time random walks (CTRW) and multi-rate mass transport (MRMT) approaches, to modeling of NOM and associated pollutants.

Please cite this article in press as: Seders Dietrich, L.A., et al., Effect of polydispersity on natural organic matter transport, Water Research (2013), http://dx.doi.org/10.1016/j.watres.2013.01.053

Acknowledgments

S.E. Silliman (Univ. Notre Dame) provided sand from the DOE site in Oyster, VA and valuable discussion. Undergraduates M. Wells and A. Thomas assisted with data collection. M. Lieberman and B. Gao performed XPS analysis of the sand (Univ. Notre Dame). The Center for Environmental Science and Technology (CEST, Univ. Notre Dame) provided use of instruments. Funding was provided by the National Science Foundation (NSF) through a graduate research fellowship (to D. McInnis, DGE-0822217) and grants EAR-0221966 and EAR-1113704. Finally, we thank three anonymous reviewers for extensive comments that greatly improved the clarity of this manuscript.

Appendix A. Supplementary data

Supplementary data related to this article can be found at http://dx.doi.org/10.1016/j.watres.2013.01.053.

REFERENCES

Aiken, G.R., McKnight, D.M., Wershaw, R.L., MacCarthy, P., 1985. An introduction to humic substances in soil, sediment, and water. In: Aiken, G.R. (Ed.), Humic Substances in Soil, Sediment, and Water: Geochemistry, Isolation, and Characterization. John Wiley & Sons, Inc, New York, pp. 1–9.

Alessi, D.S., Fein, J.B., 2010. Cadmium adsorption to mixtures of soil components: testing the component additivity approach. Chemical Geology 270, 186–195.

Angove, M.J., Johnson, B.B., Wells, J.D., 1997. Adsorption of cadmium (II) on kaolinite. Colloids and Surfaces A: Physicochemical and Engineering Aspects 126, 137–147.

Au, K.-K., Penisson, A.C., Yang, S., O'Melia, C.R., 1999. Natural organic matter at oxide/water interfaces: complexation and conformation. Geochimica et Cosmochimica Acta 63 (19–20), 2903–2917.

Avena, M.J., Koopal, L.K., 1999. Kinetics of humic acid adsorption at solid–water interfaces. Environmental Science & Technology 33, 2739–2744.

Bäckström, M., Dario, M., Karlsson, S., Allard, B., 2003. Effects of a fulvic acid on the adsorption of mercury and cadmium on goethite. The Science of the Total Environment 304, 257–268.

Bryan, N.D., Barlow, J., Warwick, P., Stephens, S., Higgo, J.J.W., Griffin, D., 2005. The simultaneous modeling of metal ion and humic substance transport in column experiments. Journal of Environmental Monitoring 7, 196–202.

Cabaniss, S.E., Zhou, Q., Maurice, P.A., Chin, Y.-P., Aiken, G.R., 2000. A log-normal distribution model for the molecular weight of aquatic fulvic acids. Environmental Science & Technology 34, 1103–1109.

Chi, F.-H., Amy, G.L., 2004. Kinetic study on the sorption of dissolved natural organic matter onto different aquifer materials: the effects of hydrophobicity and functional groups. Journal of Colloid and Interface Science 274, 380–391.

Chin, Y.-P., Aiken, G., O'Loughlin, E., 1994. Molecular weight, polydispersivity, and spectroscopic properties of aquatic humic substances. Environmental Science & Technology 28, 1853–1858.

Dagan, G., 1990. Transport in heterogeneous porous formations: spatial moments, ergodicity, and effective dispersion. Water Resources Research 26 (6), 1281–1290.

Davis, A.P., Bhatnagar, V., 1995. Adsorption of cadmium and humic acid onto hematite. Chemosphere 30, 243–256.

de Laat, A.W.M., van den Heuvel, G.L.T., 1995. Molecular weight fractionation in the adsorption of polyacrylic acid salts onto $BaTiO_3$. Colloids and Surfaces A: Physicochemical and Engineering Aspects 98, 53–59.

Dentz, M., Castro, A., 2009. Effective transport dynamics in porous media with heterogeneous retardation properties. Geophysical Research Letters 36, L03403. http://dx.doi.org/10.1029/2008GL036846.

Dentz, M., Bolster, D., 2010. Distribution- versus correlation-induced anomalous transport in quenched random velocity fields. Physical Review Letters 105, 244301.

Dobbs, R.A., Wise, R.H., Dean, R.B., 1972. The use of ultra-violet absorbance for monitoring the total organic carbon content of water and wastewater. Water Research 6, 1173–1180.

Dong, H., Onstott, T.C., DeFlaun, M.F., Fuller, M.E., Scheibe, T.D., Streger, S.H., Rothmel, R.K., Mailloux, B.J., 2002. Relative dominance of physical versus chemical effects on the transport of adhesion-deficient bacteria in intact cores from South Oyster, Virginia. Environmental Science & Technology 36, 891–900.

Dunnivant, F.M., Jardine, P.M., Taylor, D.L., McCarthy, J.F., 1992. Transport of naturally occurring dissolved organic carbon in laboratory columns containing aquifer material. Soil Science Society of America Journal 56, 437–444.

Filius, J.D., Lumsdon, D.G., Meeussen, J.C.L., Hiemstra, T., van Riemsdijk, W.H., 2000. Adsorption of fulvic acid on goethite. Geochimica et Cosmochimica Acta 64 (1), 51–60.

Floroiu, R., Davis, A.P., Torrents, A., 2001. Cadmium adsorption on aluminum oxide in the presence of polyacrylic acid. Environmental Science & Technology 35, 348–353.

Frimmel, F.H., Huber, L., 1996. Influence of humic substances on the aquatic adsorption of heavy metals on defined mineral phases. Environment International 22 (5), 507–517.

Gu, B., Mehlhorn, T.L., Liang, L., McCarthy, J.F., 1996. Competitive adsorption, displacement, and transport of organic matter on iron oxide: II. Displacement and transport. Geochimica et Cosmochimica Acta 60 (16), 2977–2992.

Guo, M., Chorover, J., 2003. Transport and fractionation of dissolved organic matter in soil columns. Soil Science 168 (2), 108–118.

Hepinstall, S.E., Turner, B.F., Maurice, P.A., 2005. Effects of siderophores on Pb and Cd adsorption to kaolinite. Clays and Clay Minerals 53, 557–563.

Huber, S.A., Frimmel, F.H., 1992. A new method for the characterization of organic carbon in aquatic systems. International Journal of Environmental Analytical Chemistry 49, 49–57.

Huber, S.A., Balz, A., Abert, M., Pronk, W., 2011. Characterization of aquatic humic and non-humic matter with size-exclusion chromatography – organic carbon detection – organic nitrogen detection (LC-OCD-OND). Water Research 45, 879–885.

Hur, J., Schlautman, M.A., 2003. Molecular weight fractionation of humic substances by adsorption onto minerals. Journal of Colloid and Interface Science 264, 313–321.

Jardine, P.M., Dunnivant, F.M., Selim, H.M., McCarthy, J.F., 1992. Comparison of models for describing the transport of dissolved organic carbon in aquifer columns. Soil Science Society of America Journal 56, 393–401.

Johnson, B.B., 1990. Effect of pH, temperature, and concentration on the adsorption of cadmium on goethite. Environmental Science & Technology 24, 112–118.

Johnson, W.P., Amy, G.L., 1995. Facilitated transport and enhanced desorption of polycyclic aromatic hydrocarbons by natural organic matter in aquifer sediments. Environmental Science & Technology 29, 807–817.

Kawasaki, N., Matsushige, K., Komatsu, K., Kohzu, A., Nara, F.W., Ogishi, F., Yahata, M., Mikami, H., Goto, T., Imai, A., 2011. Fast

and precise method for HPLC-size exclusion chromatography with UV and TOC (NDIR) detection: importance of multiple detectors to evaluate the characteristics of dissolved organic matter. Water Research 45, 6240–6248.

Kreller, D.I., Turner, B.F., Namjesnik-Dejanovic, K., Maurice, P.A., 2005. Comparison of the effects of sonolysis and γ-radiolysis on dissolved organic matter. Environmental Science & Technology 39, 9732–9737.

Liu, H., Amy, G., 1993. Modeling partitioning and transport interactions between natural organic matter and polynuclear aromatic hydrocarbons in groundwater. Environmental Science & Technology 27, 1553–1562.

Maurice, P.A., 2009. Environmental Surfaces and Interfaces from the Nanoscale to the Global Scale. John Wiley & Sons, Inc., Hoboken, New Jersey, pp. 210–214.

Maurice, P.A., Pullin, M.J., Cabaniss, S.E., Zhou, Q., Namjesnik-Dejanovic, K., Aiken, G.R., 2002. A comparison of surface water natural organic matter in raw filtered water samples, XAD, and reverse osmosis isolates. Water Research 36, 2357–2371.

Maurice, P.A., Anthony, C., Arthurs, L., Giesting, P., Golden, S., Hepinstall, S., Liu, G., Lavarnway, A., Mishra, B., Tholen, K., 2004. Effects of Cd on natural organic matter adsorption to goethite. Water–Rock Interaction International XI, 1331–1334.

McCarthy, J.F., Williams, T.M., Liang, L., Jardine, P.M., Jolley, L.W., Taylor, D.L., Palumbo, A.V., Cooper, L.W., 1993. Mobility of natural organic matter in a sandy aquifer. Environmental Science & Technology 27, 667–676.

McCarthy, J.F., Gu, B., Liang, L., Mas-Pla, J., Williams, T.M., Yeh, T.-C.J., 1996. Field tracer tests on the mobility of natural organic matter in a sandy aquifer. Water Resources Research 32, 1223–1238.

McCarthy, J.F., Czerwinski, K.R., Sanford, W.E., Jardine, P.M., Marsh, J.D., 1998. Mobilization of transuranic radionuclides by natural organic matter. Journal of Contaminant Hydrology 30, 49–77.

McKnight, D.M., Bencala, K.E., Zellweger, G.W., Aiken, G.R., Feder, G.L., Thorn, K.A., 1992. Sorption of dissolved organic carbon by hydrous aluminum and iron oxides occurring at the confluence of Deer Creek with the Snake River, Summit County, Colorado. Environmental Science & Technology 26, 1388–1396.

Meier, M., Namjesnik-Dejanovic, K., Maurice, P.A., Chin, Y.-P., Aiken, G.R., 1999. Fractionation of aquatic natural organic matter upon sorption to goethite and kaolinite. Chemical Geology 157, 275–284.

Münch, J.-M., Totsche, K.U., Kaiser, K., 2002. Physicochemical factors controlling the release of dissolved organic carbon from columns of forest subsoils. European Journal of Soil Science 53, 311–320.

Namjesnik-Dejanovic, K., Maurice, P.A., Aiken, G.R., Cabaniss, S., Chin, Y.-P., Pullin, M.J., 2000. Adsorption and fractionation of a muck fulvic acid on kaolinite and goethite at pH 3.7, 6, and 8. Soil Science 165 (7), 545–559.

Pullin, M.J., Progess, C.A., Maurice, P.A., 2004. Effects of photoirradiation on the adsorption of dissolved organic matter to goethite. Geochimica et Cosmochimica Acta 68 (18), 3643–3656.

Saito, T., Koopal, L.K., van Riemsdijk, W.H., Nagasaki, S., Tanaka, S., 2004. Adsorption of humic acid on goethite: isotherms, charge adjustments, and potential profiles. Langmuir 20, 689–700.

Schlautman, M.A., Morgan, J.J., 1994. Adsorption of aquatic humic substances on colloidal-size aluminum oxide particles: influence of solution chemistry. Geochimica et Cosmochimica Acta 58 (20), 4293–4303.

Sun, L., Perdue, E.M., McCarthy, J.F., 1995. Using reverse osmosis to obtain organic matter from surface and ground waters. Water Research 29 (6), 1471–1477.

Tipping, E., 1981. The adsorption of aquatic humic substances by iron oxides. Geochimica et Cosmochimica Acta 45, 191–199.

Traina, S.J., Novak, J., Smeck, N.E., 1990. An ultraviolet absorbance method of estimating the percent aromatic carbon content of humic acids. Journal of Environmental Quality 19, 151–153.

van de Weerd, H., van Riemsdijk, W.H., Leijnse, A., 1999. Modeling the dynamic adsorption/desorption of a NOM mixture: effects of physical and chemical heterogeneity. Environmental Science & Technology 33, 1675–1681.

van de Weerd, H., van Riemsdijk, W.H., Leijnse, A., 2002. Modeling transport of a mixture of natural organic molecules: effects of dynamic competitive sorption from particle to aquifer scale. Water Resources Research 38, 1158.

Vermeer, A.W.P., van Riemsdijk, W.H., Koopal, L.K., 1998. Adsorption of humic acid to mineral particles. 1. Specific and electrostatic interactions. Langmuir 14, 2810–2819.

Vermeer, A.W.P., McCulloch, J.K., van Riemsdijk, W.H., Koopal, L.K., 1999. Metal ion adsorption to complexes of humic acid and metal oxides: deviations from the additivity rule. Environmental Science & Technology 33, 3892–3897.

Wei, X., Shao, M., Horton, R., Han, X., 2010. Humic acid transport in water-saturated porous media. Environmental Modeling & Assessment 15, 53–63.

Weigand, H., Totsche, K.U., 1998. Flow and reactivity effects on dissolved organic matter transport in soil columns. Soil Science Society of America Journal 62 (5), 1268–1274.

Weng, L., van Riemsdijk, W.H., Koopal, L.K., Hiemstra, T., 2006. Adsorption of humic substances on goethite: comparison between humic acids and fulvic acids. Environmental Science & Technology 40, 7494–7500.

Zhou, Q., Cabaniss, S.E., Maurice, P.A., 2000. Considerations in the use of high-pressure size exclusion chromatography (HPSEC) for determining molecular weights of aquatic humic substances. Water Research 34 (14), 3505–3514.

Zhou, Q., Maurice, P.A., Cabaniss, S.E., 2001. Size fractionation upon adsorption of fulvic acid on goethite: equilibrium and kinetic studies. Geochimica et Cosmochimica Acta 65 (5), 803–812.

Please cite this article in press as: Seders Dietrich, L.A., et al., Effect of polydispersity on natural organic matter transport, Water Research (2013), http://dx.doi.org/10.1016/j.watres.2013.01.053